Two-dimensional electron gas at manganite buffered $LaAlO_3/SrTiO_3$ (001) interface by spin coating chemical methods

Tahira Khan, Hongrui Zhang, Hui Zhang, Zhihuan Yang, Jinghua Song, Jine Zhang, Xiaobing Chen, Yuansha Chen, Baogen Shen, and Jirong Sun

Citation: Appl. Phys. Lett. **113**, 071601 (2018); doi: 10.1063/1.5044626
View online: https://doi.org/10.1063/1.5044626
View Table of Contents: http://aip.scitation.org/toc/apl/113/7
Published by the American Institute of Physics

Two-dimensional electron gas at manganite buffered $LaAlO_3/SrTiO_3$ (001) interface by spin coating chemical methods

Tahira Khan, Hongrui Zhang, Hui Zhang, Zhihuan Yang, Jinghua Song, Jine Zhang, Xiaobing Chen, Yuansha Chen, Baogen Shen, and Jirong Sun[a)]
Beijing National Laboratory for Condensed Matter and Institute of Physics, Chinese Academy of Sciences, Beijing 100190, People's Republic of China and School of Physical Sciences, University of Chinese Academy of Sciences, Beijing 100190, People's Republic of China

(Received 14 June 2018; accepted 27 July 2018; published online 13 August 2018)

High mobility spin-polarized two-dimensional electron gas (2DEG) is crucially important for spintronic applications. Here, we report our investigations on the 2DEG fabricated by spin coating a $LaAlO_3$ layer on a (001) $SrTiO_3$ substrate with a $La_{2/3}Sr_{1/3}MnO_3$ buffer layer. When the buffer layer is below 3 uc, the 2DGE is highly mobile. Corresponding to the layer thicknesses of 0, 1, and 2 uc, the Hall mobilities are $\sim$24 000 cm^2/V s, $\sim$28 000 cm^2/V s, and $\sim$59 600 cm^2/V s at 2 K. In contrast, the 2DEG with a buffer layer of 3 uc shows a relatively low mobility ($\sim$3000 cm^2/V s). However, an anomalous Hall effect was observed in this 2DEG below 20 K, indicating a long range ferromagnetic order. This work demonstrates the great potential of the chemical method in gaining high quality spin-polarized 2DEGs at the $LaAlO_3/SrTiO_3$ interface. *Published by AIP Publishing.*
https://doi.org/10.1063/1.5044626

Two-dimensional electron gas (2DEG) at the $LaAlO_3/SrTiO_3$ (LAO/STO) interface has attracted great attention due to its unique characteristics like high mobility, low temperature superconductivity, ferromagnetism, and the coexistence of the latter two features, which is quite rare in other systems.[1–17] Despite intensive investigations, highly mobile and ferromagnetic 2DEG is still strongly desired to make the 2DEG a candidate for next generation spintronic applications.[18–20]

In order to enhance the ferromagnetism at the LAO/STO interface, interface decoration by a buffer layer of some ferromagnetic oxides is adopted, e.g., inserting a 1-uc $EuTiO_3$ layer between LAO and STO has been proved successful for yielding spin-polarized 2DEG below a temperature of 8 K, as evidenced by the appearance of a prominent anomalous Hall effect (AHE).[17,21,22] Other than the LAO/STO interface, a signature of ferromagnetism was also observed in the $NdGaO_3/SrTiO_3$ interface, suggesting that 10 K is the highest temperature for the AHE.[23] Inserting a 1-uc crystalline $La_xSr_{1-x}MnO_3$ ($x = 1/3$ and 1/8) buffer layer has been found to greatly enhance the mobility of the 2DEG, but it is unable to make the interface ferromagnetic. Inserting a thick $La_xSr_{1-x}MnO_3$ buffer layer, which may improve interfacial ferromagnetism, always makes the interface insulating. Recently, it was found that when the $La_xSr_{1-x}MnO_3$ ($x = 1/8$) buffer layer is initially amorphous and crystallized during the deposition process of the LAO top layer, a spin polarized interface can be gained.[24]

In all of the above reports, the samples are prepared by pulsed laser deposition (PLD). In our previous report, we have demonstrated the formation of high quality 2DEGs at the LAO/STO interfaces using spin coating chemical methods.[26] In this work, we will perform a systematic study on the effect of the $La_xSr_{1-x}MnO_3$ (LSMO, $x = 1/3$) buffer layer on the 2DEGs when the top LAO layer is prepared by the spin coating chemical methods. We have obtained 2DEGs with the mobility as high as 59 500 cm^2/V s in the presence of a LSMO buffer layer of 1 or 2 uc and observed signatures of long-range ferromagnetic order when the buffer layer is 3 uc.

LAO/LSMO/STO samples with a LSMO buffer layer of 0, 1, 2, and 3 uc were grown with the following procedures: At first, a crystalline LSMO layer was grown on a TiO_2-terminated (001)-STO substrate ($5 \times 5 \times 0.5\ mm^3$) at 650 °C under the O_2 pressure of 2.7×10^{-5} mbar. The growth process was monitored by reflected high energy electron diffraction (RHEED). The laser pulse fluence was 1.5 J/cm^2, and the repetition rate was 1 Hz (wavelength = 248 nm). After deposition, the sample was cooled to room temperature at a rate of 10 °C/min without changing the deposition oxygen pressure. Later on, the LAO film was grown by the spin coating chemical methods following the procedures below: A droplet of the precursor, 0.01 mole solution of lanthanum nitrate hydrate $La(NO_3)_3 \cdot 9H_2O$, aluminum nitrate nanohydrate $Al(NO_3)_3 \cdot 9H_2O$, N,N-dimethylformamide (DMF), polyvinylpyrrolidone (PVP), and deionized water, was dripped on a STO substrate and was spread smoothly by first spinning at 300 rpm for 15 s following by a spinning at 7000 rpm for 60 s. The film thus obtained was subsequently annealed in air for 3 h at 450 °C to crystalize the LAO film and then at 700 °C for 10 min in a high vacuum atmosphere of 10^{-4} Pa to form a conducting interface. Further details can be found elsewhere.[26]

The surface morphology of the film was measured by atomic force microscopy (AFM, SPI 3800N, Seiko). The film thickness was determined by x-ray reflectivity (XRR) conducted using a Bruker diffractometer (D8 Discover with Cu Kα radiation). Resistive measurements were conducted using a Quantum-Designed physical property measurement system (PPMS) with an applied current of 10 μA. The van der Pauw geometry was adopted for resistive measurements, and ultrasonic Al wire bonding was used for electric contacts.

[a)]Author to whom correspondence should be addressed: jrsun@iphy.ac.cn

Figure 1(a) shows the RHEED intensity as a function of time, recorded in the growth process of LSMO. The clear oscillation indicates a layer-by-layer growth of the LSMO film on STO, and the layer thicknesses are ~1, 2, and 3 uc, respectively. Figure 1(b) presents RHEED patterns of the bare STO and the LSMO of 3 uc on STO. Sharp reflection spots indicate the high surface quality of both samples. Figures 1(c) and 1(d) are the AFM image and line profile of the LSMO (3 uc)/STO sample, exhibiting regular surface terraces with a step height of 0.4 nm and a step width of 270 nm. The AFM image shown here is taken for the LSMO buffer layer. It indicates a uniform growth of LSMO on the STO substrate. Figure 1(e) shows the surface morphology of the LAO film grown on the LSMO (3 uc)/STO sample. The LAO top layer looks smooth and has a root mean-squared roughness (RMS) of 1.2 nm. Figure 1(f) shows X-ray reflectivity (XRR) of the sample with the LAO layer, and regular oscillations indicate the smoothness of the LAO film. Fitting to the XRR spectrum gives a thickness of approximately ~15 nm for the LAO film.

Figure 2(a) shows the sheet resistance of the 2DEGs at the LAO/LSMO/STO interfaces. All samples exhibit a metallic behavior. Compared with 2DEG without the LSMO buffer layer, fascinatingly, the conduction of 2DEGs at the LAO/LSMO/STO interfaces is considerably enhanced when the LSMO layer thickness is 1 and 2 uc. The sheet resistance at 2 K reduces from 2.46 Ω/□ to 0.66 Ω/□ and to 0.33Ω/□

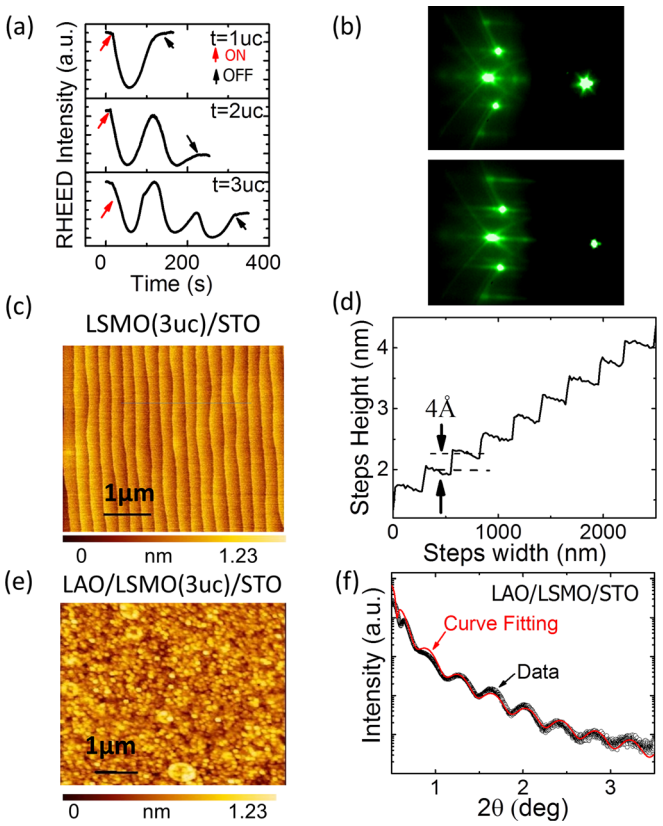

FIG. 1. (a) RHEED intensity for the deposition of various unit cells of crystalline $La_xSr_{1-x}MnO_3$ (x = 1/3) buffer layer. (b) RHEED pattern of the STO (001) substrate before and after deposition of the LSMO layer with t = 3 uc. (c) and (d) AFM images of STO (001) after deposition of LSMO (3 uc) and a line profile, respectively. (e) Surface morphology and (d) XRR of LAO/LSMO (3 uc)/STO (001).

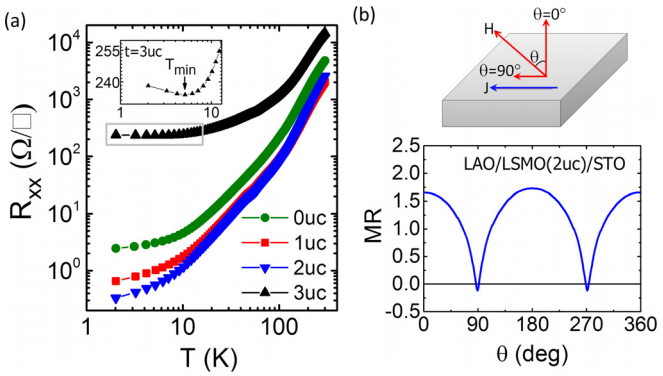

FIG. 2. (a) Sheet resistance as a function of temperature. (b) Sketch for the measurement of magneto-resistance and magneto-resistance MR as a function of sample position with respect to field at 2 K under an applied magnetic field of 7 T.

as the LSMO layer thickness increases from 0 to 2 uc. Correspondingly, the R_S(300 K)/R_S(2 K) ratio, which is a characterization of the metallicity of the 2DEGs, is as high as ~1948, ~3124, and ~7748. In contrast, the sheet resistance of LAO/LSMO (3 uc)/STO is significantly increased by the introduction of LSMO, increasing to 233.20 Ω/□ at 2 K. The R_S(300 K)/R_S(2 K) ratio is ~62. Particularly, a slight resistance upturn appears below 5 K, indicating the occurrence of the Kondo effect (marked as an arrow). In order to confirm the nature of the electron gas formed at the interface, we have performed magneto-resistance measurements at 2 K under an applied magnetic field of 7 T. Figure 2(b) is the sketch for the measurement of magneto-resistance and magneto-resistance magnetoresistance (MR) (%) as a function of sample position with respect to the field for LAO/LSMO (2 uc)/STO. The type of MR anisotropy observed here is the typical behavior of purely 2DEG formed at the interface as described in the literature.[27] For 2DEG, magnetoresistance (MR) is maximum for perpendicular magnetic field H and zero for in-plane magnetic field H, the same as a rectified sine wave,[28] whereas 3D samples show a sine wave behavior with angular rotation of the sample position in the magnetic field.[27]

Figures 3(a)–3(d) present the Hall resistance (R_{xy}) of the samples with different LSMO buffer layers, as a function of magnetic field (H). The Hall resistance is very linear against the magnetic field when the LSMO layer is 0, 1, and 2 uc in thickness. This is an indication of only one species of charge carrier in the 2DEGs. Moreover, the R_{xy}-H slope is nearly constant with the change of temperature, indicating that the carrier density is temperature-independent. This is an indication of high quality 2DEG without charge localization even at low temperatures.

An obviously different Hall effect is observed for the sample with a 3-uc-thick buffer layer. As shown in Fig. 3(d), at high temperature, R_{xy} varies linearly with the applied magnetic field, which is the typical behavior of the normal Hall effect. However, when the sample is cooled down to 30 K, bending in the R_{xy}-H curve initiates around $H = 0$ and becomes even obvious upon further cooling to 2 K. Particularly, strong curve bending mainly appears in the low-field range ($|H| < 2$ T). Such a curvature cannot be described by the two-band model in contrast to the LAO/STO interface.[23,25] Although the two-band model fit looks very well at temperatures 20 K and below

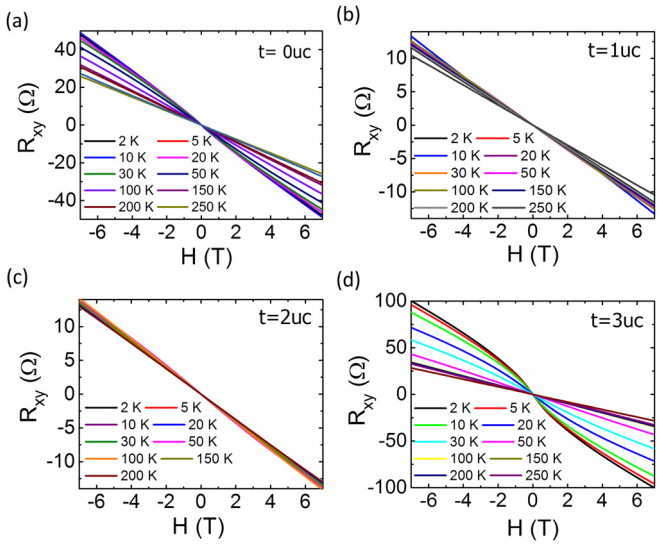

FIG. 3. (a)–(d) Hall characteristics for samples with various LSMO buffer layers.

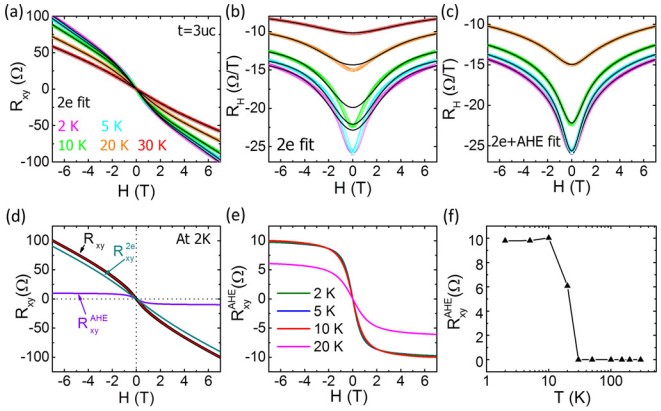

FIG. 4. (a) Experimental (thick lines) and calculated (black lines) Hall resistances of the sample for LAO/LSMO (3 uc)/STO (001), obtained at low temperatures. (b) and (c) Differential of R_{xy} with respect to H. Colored lines are experimental results and black lines are results of two-band model and extended two-band model fitting. (d) A comparison of the total Hall effect with R_{xy}^{2e} and R_{xy}^{AHE}, depicted as functions of magnetic field at 2 K. Thick black and thin red lines are measured and fitted results, respectively. The purple line marks the deduced R_{xy}^{AHE} and dark cyan corresponds to R_{xy}^{2e}. (e) Anomalous Hall resistance as a function of magnetic field at different temperatures. (f) Anomalous Hall resistance as a function of temperature, recorded at 7 T. The solid line is a guide to the eye.

[Fig. 4(a)], a clear deviation from the experimental results can be observed around zero field when the results are plotted in the form of $dR_H = dR_{xy}/dH$ [Fig. 4(b)]. We obtained good two band model fitting only at 30 K. To investigate the non-linear Hall effect below 20 K, the Hall coefficient defined by the differential of R_{xy} with respect to H is only reproducible by an extended two-band model which includes a normal Hall resistance R_{xy}^{2e} and an anomalous Hall resistance R_{xy}^{AHE} (we did not consider the holes in the LSMO layer since the latter is insulating when its thickness is equal to or below 3 uc)

$$R_{xy} = R_{xy}^{2e} + R_{xy}^{AHE}, \tag{1}$$

where

$$R_{xy}^{2e} = -\frac{1}{e}\frac{\left(\frac{n_1\mu_1^2}{1+\mu_1^2H^2} + \frac{n_2\mu_2^2}{1+\mu_2^2H^2}\right)H}{\left(\frac{n_1\mu_1^2}{1+\mu_1^2H^2} + \frac{n_2\mu_2^2}{1+\mu_2^2H^2}\right)^2 + \left(\frac{n_1\mu_1^2}{1+\mu_1^2H^2} + \frac{n_2\mu_2^2}{1+\mu_2^2H^2}\right)^2 H^2}, \tag{2}$$

which is constrained by

$$R_{xx}^{-1}(H=0) = e(n_1\mu_1 + n_2\mu_2) \tag{3}$$

and

$$R_{xy}^{AHE} = \alpha L\left(\frac{mH}{k_BT}\right), \tag{4}$$

with $L(x)$ being defined as $L(x) = \coth(x) - \frac{1}{x}$.[23]

In these equations, n_1 and n_2 are the densities of two species of charge carriers, and μ_1 and μ_2 are the corresponding Hall mobilities. They can be determined by fitting the experimental data to Eq. (1). To fit to nonlinear Hall data, one might consider more than two electron populations, but it cannot yield good fit when the anomalous Hall effect appears as described by Ref. 29 where even ten electron populations cannot retrace a good fit, particularly, at low fields.

On the basis of data fitting, the two Hall components R_{xy}^{2e} and R_{xy}^{AHE} can be determined and displayed as functions of magnetic field [Fig. 4(d)]. Here, we can observe the opposite sign of R_{xy}^{AHE} with the field, i.e., for positive field H, R_{xy}^{AHE} is negative similar to LAO/LSMO (1 nm)/STO.[24] This sign is opposite to that obtained for $NdGaO_3/SrTiO_3$ or LAO/$EuTiO_3$/STO where AHE exhibits the same sign as of field H.[17,21] It can be concluded that the opposite sign for R_{xy}^{AHE} is due to spin polarization in the opposite direction. Figure 4(e) shows the field-dependent R_{xy}^{AHE} obtained in the temperature range from 2 K to 20 K. At first glance, R_{xy}^{AHE} is considerably large at low temperatures. It is ~10 Ω at 2 K, which is about 10% for the total Hall resistance at 7 T. As expected, R_{xy}^{AHE} changes drastically at lower fields but saturates at high fields. This is the typical feature of AHE. It means a rapid increase in the magnetization of 2DEG before saturation at high fields. In Fig. 4(f), we display the saturated R_{xy}^{AHE} as a function of temperature. An AHE signal starts at 20 K, develops rapidly upon further cooling, and saturates below 10 K. The ultrathin LSMO buffer layer is insulating. Therefore, the anomalous Hall signal originates mainly from 2DEG of the

STO interface underneath LSMO. Generally, asymmetric scattering of charge carriers from magnetic centers contributes to AHE in ferromagnetic materials. The presence of AHE in our sample provides evidences for the presence of long range ferromagnetic orders and spin polarization in LSMO buffered 2DEGs. Compared to other systems such as $NdGaO_3/SrTiO_3$ and $LAO/EuTiO_3/STO$ where AHE appears below 10 K,[17,21] the ordering temperature in our 2DEG is obviously high (20 K).[17,21] As for the 1-uc and 2-uc-thick buffer layers, they are too thin to produce any sizable effect on AHE, which is consistent with the conclusion of the previous report.[17]

Figure 5(a) shows variations in carrier density with temperature for different samples. From 0 to 3 uc, the carrier density is correspondingly $\sim 1.0 \times 10^{14}\,cm^{-2}$, $\sim 4.0 \times 10^{14}\,cm^{-2}$, $4.1 \times 10^{14}\,cm^{-2}$, and $\sim 1.5 \times 10^{14}\,cm^{-2}$ at 300 K. It is obviously higher for the 1-uc- and 2-uc-thick samples than for the 0 and 3-uc-thick samples. The decrease in carrier density for the 3-uc-LSMO-buffered 2DEG is expectable since the LSMO layer has blocked the charge transfer from LAO to STO. The low carrier density in un-buffered 2DEG could be ascribed to the unsatisfactory interface state.

With the decrease in temperature, carrier density displays a slow decrease especially for the 0 and the 3-uc-LSMO 2DEGs, indicating a gradual freezing of the mobile carriers. When temperature is lower than 30 K, the Hall effect of the 3-uc 2DEG has to be described by the two band model, i.e., a second species of charge carrier emerges, and its density (n_2) experiences a rapid growth when cooled from 30 K down to 10 K. According to Fig. 5(a), n_2 is $\sim 6.25 \times 10^{11}\,cm^{-2}$ at 30 K and $\sim 1.8 \times 10^{12}\,cm^{-2}$ at 2 K, showing a more than 3-fold increment. Compared with n_2, n_1 is much larger. It is generally on the order of $\sim 5.68 \times 10^{13}\,cm^{-2}$ even at low temperatures. Corresponding to the rapid increase in n_2, fascinatingly, n_1 shows an obvious decrease by a value much larger than the increment in n_2. Presumably, the rapid freezing of n_1 and the appearance of n_2 have a relation that is still not clear at present.

Figure 5(b) shows the mobility for the samples with various buffer layers, as a function of temperature. Corresponding to the LSMO thickness of 0, 1, and 2 uc, the mobility is ~8, ~7, and ~6 $cm^2/V\,s$ at 300 K and it is ~28 000, ~24 000, and ~59 600 $cm^2/V\,s$ at 2 K. By introducing the LSMO buffer layer of 2 uc, we have promoted the mobility to nearly 6×10^4 $cm^2/V\,s$. This value is comparable with the highest mobility reported until now.[17] However, the 3-uc sample exhibits a different behavior. The mobility of the majority charge carrier is very low, $\mu_1 \sim 397\,cm^2/V\,s$ at 2 K, though it shares the same temperature dependence with other three samples. It is possible that interlayer diffusion has taken place between LSMO and STO, slowing down the charge carriers. Presumably, it is this interlayer diffusion that establishes the magnetic order in 2DEG. An interesting observation is the temperature independence of the mobility of the minority charge carriers. As shown in Fig. 5(b), μ_2 is nearly constant in the temperature range from 30 K down to 2 K. It means that the effect of phonon scattering and the change in permittivity of STO is weak on the species of charge carriers. Moreover, μ_2 is much larger than μ_1, as high as $2050\,cm^2/V\,s$ at 2 K. Normally, these fast and slow charge carriers are d_{YZ}/d_{ZX} and d_{XY} electrons. Compared with the d_{YZ}/d_{ZX} electrons, the d_{XY} electrons populate near the interface and thus suffer from strong interfacial scattering. Since n_1 is much greater than n_2, the ferromagnetic order in the 2DEG may be mediated by the first species of charge carriers. Of course, further investigations in this aspect are required.

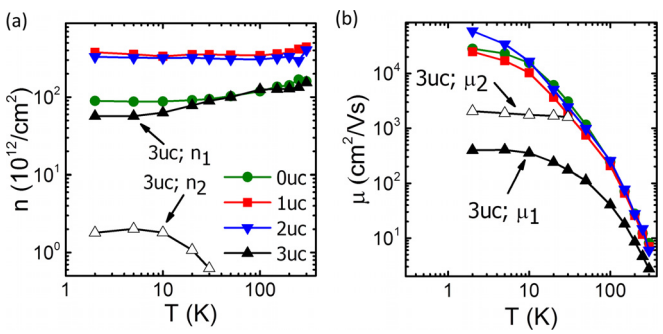

FIG. 5. (a) Carrier density and (b) mobility of carriers with temperature for LAO/LSMO/STO (001) with various thicknesses of the LSMO buffer layer. In (a) and (b), two kinds of populations for LSMO ~3 uc are obtained from data fits to Hall characteristics, which leads to two different mobilities.

In summary, high mobility spin-polarized two-dimensional electron gas (2DEG) is fabricated by spin coating a $LaAlO_3$ layer on a (001) $SrTiO_3$ substrate with a $La_{2/3}Sr_{1/3}$ MnO_3 buffer layer. A highly mobile 2DEG is obtained when the buffer layer is below 3 uc. However, an anomalous Hall effect was observed in this 2DEG below 20 K, indicating a long range ferromagnetic order. Anisotropic magneto-resistance measurements provide confirmation for the formation of the 2DEG at the interface. This work demonstrates the great potential of the chemical method in gaining high quality spin-polarized 2DEGs at the $LaAlO_3/SrTiO_3$ interface.

This work was supported by the National Basic Research of China (Nos. 2016YFA0300701, 2017YFA0206300, and 2017YFA0303601), the National Natural Science Foundation of China (Nos. 11520101002, 51590880, and 11674378), and the Key Program of the Chinese Academy of Sciences.

[1]A. Ohtomo and H. Y. Hwang, Nature **427**, 423–426 (2004).
[2]N. Reyren, S. Thiel, A. D. Caviglia, L. F. Kourkoutis, G. Hammeri, C. Richter, C. W. Schneider, T. Kopp, A. S. Ruetschi, D. Jaccard, M. Gabay, D. A. Muller, J. M. Triscone, and J. Mannhart, Science **317**, 1196–1199 (2007).
[3]S. Gariglio, N. Reyren, A. D. Caviglia, and J. M. Triscone, J. Phys.: Condens. Matter **21**, 164213 (2009).
[4]A. Brinkman, M. Huijben, M. Van Zalk, J. Huijben, U. Zeitler, J. C. Maan, W. G. V. D. Wiel, G. Rijnders, D. H. A. Blank, and H. Hilgenkamp, Nat. Mater. **6**, 493–496 (2007).
[5]J. A. Bert, B. Kalisky, C. Bell, M. Kim, Y. I. Hikita, H. Y. Hwang, and K. A. Moler, Nat. Phys. **7**, 767–771 (2011).
[6]H. Y. Hwang, Y. Iwasa, M. Kawasaki, B. Keimer, N. Nagaosa, and Y. Tokura, Nat. Mater. **11**, 103–113 (2012).
[7]A. D. Caviglia, S. Gariglio, C. Cancellieri, B. Sacépé, A. Fête, N. Reyren, M. Gabay, A. F. Morpurgo, and J.-M. Triscone, Phys. Rev. Lett. **105**, 236802 (2010).
[8]A. D. Caviglia, S. Gariglio, N. Reyren, D. Jaccard, T. Schneider, M. Gabay, S. Thiel, G. Hammerl, J. Mannhart, and J.-M. Triscone, Nature (London) **456**, 624–627 (2008).
[9]A. D. Caviglia, M. Gabay, S. Gariglio, N. Reyren, C. Cancellieri, and J.-M. Triscone, Phys. Rev. Lett. **104**, 126803 (2010).
[10]Y. W. Xie, C. Bell, T. Yajima, Y. Hikita, and H. Y. Hwang, Nano Lett. **10**, 2588–2591 (2010).

[11]S. Thiel, G. Hammerl, A. Schmehl, C. W. Schneider, and J. Mannhart, Science **313**, 1942–1945 (2006).
[12]C. Cen, S. Thiel, G. Hammerl, C. W. Schneider, K. E. Andersen, C. S. Hellberg, J. Mannhart, and J. Levy, Nat. Mater. **7**, 298–302 (2008).
[13]C. Bell, S. Harashima, Y. Kozuka, M. Kim, B. G. Kim, Y. Hikita, and H. Y. Hwang, Phys. Rev. Lett. **103**, 226802 (2009).
[14]E. Lesne, Y. Fu, S. Oyarzun, J. C. Rojas-Sánchez, D. C. Vaz, H. Naganuma, G. Sicoli, J.-P. Attané, M. Jamet, E. Jacquet, J.-M. George, A. Barthélémy, H. Jaffrès, A. Fert, M. Bibes, and L. Vila, Nat. Mater. **15**, 1261–1266 (2016).
[15]M. Huijben, G. Koster, M. K. Kruize, S. Wenderich, J. Verbeeck, S. Bals, E. Slooten, B. Shi, H. J. A. Molegraaf, J. E. Kleibeuker, S. van Aert, J. B. Goedkoop, A. Brinkman, D. H. A. Blank, M. S. Golden, G. van Tendeloo, H. Hilgenkamp, and G. Rijnders, Adv. Funct. Mater. **23**, 5240–5248 (2013).
[16]Y. W. Xie, C. Bell, Y. Hikita, S. Harashima, and H. Y. Hwang, Adv. Mater. **25**, 4735–4738 (2013).
[17]Y. Z. Chen, F. Trier, T. Wijnands, R. J. Green, N. Gauquelin, R. Egoavil, D. V. Christensen, G. Koster, M. Huijben, N. Bovet, S. Macke, F. He, R. Sutarto, N. H. Andersen, J. A. Sulpizio, M. Honig, G. E. D. K. Prawiroatmodjo, T. S. Jespersen, S. Linderoth, S. Ilani, J. Verbeeck, G. Van Tendeloo, G. Rijnders, G. A. Sawatzky, and N. Pryds, Nat. Mater. **14**, 801 (2015).
[18]Ariando, X. Wang, G. Baskaran, Z. Q. Liu, J. Huijben, J. B. Yi, A. Annadi, A. Roy Barman, A. Rusydi, S. Dhar, Y. P. Feng, J. Ding, H. Hilgenkamp, and T. Venkatesan, Nat. Commun. **2**, 188 (2011).
[19]F. Bi, M. C. Huang, S. Ryu, H. Lee, C. W. Bark, C. B. Eom, P. Irvin, and J. Levy, Nat. Commun. **5**, 5019 (2014).
[20]J.-S. Lee, Y. W. Xie, H. K. Sato, C. Bell, Y. Hikita, H. Y. Hwang, and C.-C. Kao, Nat. Mater. **12**, 703 (2013).
[21]F. Trier, G. E. D. K. Prawiroatmodjo, Z. Zhong, D. V. Christensen, M. von Soosten, A. Bhowmik, J. M. G. Lastra, Y. Chen, T. S. Jespersen, and N. Pryds, Phys. Rev. Lett. **117**, 096804 (2016).
[22]D. Stornaiuolo, C. Cantoni, G. M. D. Luca, R. D. Capua, E. D. Gennaro, G. Ghiringhelli, B. Jouault, D. Marrè, D. Massarotti, F. M. Granozio, I. Pallecchi, C. Piamonteze, S. Rusponi, F. Tafuri, and M. Salluzzo, Nat. Mater. **15**, 278 (2016).
[23]F. Gunkel, C. Bell, H. Inoue, B. Kim, A. G. Swartz, T. A. Merz, Y. Hikita, S. Harashima, H. K. Sato, M. Minohara, S. Hoffmann-Eifert, R. Dittmann, and H. Y. Hwang, Phys. Rev. X **6**, 031035 (2016).
[24]H. R. Zhang, Y. Zhang, H. Zhang, J. Zhang, X. Shen, X. X. Guan, Y. Z. Chen, R. C. Yu, N. Pryds, Y. S. Chen, B. G. Shen, and J. R. Sun, Phys. Rev. B **96**, 195167 (2017).
[25]A. Joshua, S. Pecker, J. Ruhman, E. Altman, and S. Ilani, Nat. Commun. **3**, 1129 (2012).
[26]T. Khan, H. Zhang, H. R. Zhang, X. Yan, D. S. Hong, F. R. Han, Y. S. Chen, B. G. Shen, and J. R. Sun, Nanotechnology **28**, 435701 (2017).
[27]W. N. Lin, J. F. Ding, S. X. Wu, Y. F. Li, J. Lourembam, S. Shannigrahi, S. J. Wang, and T. Wu, Adv. Mater. Interfaces **1**, 1300001 (2014).
[28]X. Wang, W. M. Lü, A. Annadi, Z. Q. Liu, K. Gopinadhan, S. Dhar, T. Venkatesan, and Ariando, Phys. Rev. B **84**, 075312 (2011).
[29]N. M. Nemes, M. J. Calderón, J. I. Beltrán, F. Y. Bruno, J. García-Barriocanal, Z. Sefrioui, C. León, M. García-Hernández, M. C. Muñoz, L. Brey, and J. Santamaría, Adv. Mater. **26**, 7516–7520 (2014).